IEEE Transactions on Plasma Science; Volume: 39, Issue: 10, p 1974 – 1982

An Improved Local Thermal Equilibrium Model of DC Arc Plasma Torch

R. Huang and H. Fukanuma, Plasma Giken Co., Ltd., Tokyo, Japan
Y. Uesugi and Y. Tanaka, Kanazawa University, Kanazawa City, Japan

Abstract

Most of the simulation models about arc plasma are based on the hypothesis of Local Thermal Equilibrium (LTE). The non-equilibrium model is very complicated due to the calculation of electron temperature. In this study, an improved LTE model is developed and applied to the three-dimensional simulation of the flow patterns inside a non-transferred DC arc plasma torch. Numerical calculations on the distribution of gas temperature and velocity in the plasma torch were carried out using argon as the plasma gas. The electric current density and potential are also discussed. The results indicate that the temperature and velocity distributions of arc are almost axisymmetrical. The results of voltage drop agree well with the experiment observations. It seems that anode erosion is located on the internal surface of the anode, where the largest number of electrons are injected.

Index Terms-plasma spraying, plasma torch, local thermal equilibrium, three-dimensional modeling.

Nomenclature

ρ	Gas mass density	B	Magnetic induction vector
V	Gas velocity	P	Gas pressure
t	Time	μ	Dynamic viscosity
j	Electric current density vector	S	Strain rate tensor
cp	Specific heat at constant pressure	T	Gas temperature
E	Electric field	Sr	Volumetric net radiation losses
λ	Gas thermal conductivity	σ	Electric conductivity
⌀	Electric potential	A	Magnetic vector potential
$\mu 0$	Permeability of free space	Rg	Gas constant
Te	Nominal electron temperature	mh	Mass of heavy particle
me	Mass of electron	e	Elementary charge
λe	Free path of electron	k	Boltzmann constant
nh	Number density of heavy particles	ne	Number density of electrons

I. INTRODUCTION

Plasma spraying is widely used in industrial fields to provide coatings for protection of materials against wear, erosion, corrosion and thermal loads based on a high heat source with temperature over 10000K enough to melt any material at atmospheric pressure. Since the appearance of industrial DC arc plasma spray torches in the 1960s, the research of this field through both measurements and modeling has been extensively conducted [1]. In recent years, although a number of robust, user friendly particle diagnostic tools have become available for plasma spray processes to assess the in-flight particle temperature, velocity, trajectory and particle diameter distributions, it is still difficult to observe the complex properties of arc inside a plasma torch [2].

A conventional DC non-transferred plasma torch (representing more than 90% of industrial torches) with a stick-type cathode is shown schematically in figure 1 [3-4]. After the working gas enters the torch, it is heated by an electric arc formed between a nozzle-shaped anode and a conical cathode, and ejected as a jet. Particles to be plasma sprayed are fed into the particle inlet, heated and accelerated within the plasma jet by the working gas via the plasma arc. The experimental research performed on the plasma arc is mainly concentrated on the measurement of arc voltage [3-6], arc behavior at the torch exit and observation of the jet formed by the plasma torch [3]. S. Goutier et al. also measured the particle temperature fluctuations [7]. Few of the reports about the arc behavior inside the torch present experimental results, due to the equipment limitations.

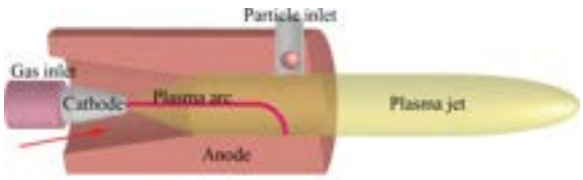

Fig. 1. Schematic of a conventional DC arc torch

Fortunately, numerical calculation provides a valid way to understand arc behavior inside the plasma torch. The modeling of DC arc plasma torches is an extremely challenging task because the plasma flow is highly nonlinear and presents strong property gradients. It is characterized by a wide range of time and length scales, and often includes chemical and

thermodynamic non-equilibrium effects, especially near its boundaries [8]. Despite of the complexity of the subject, over the past few decades, many papers concerning numerical studies of the characteristics of DC arc plasma torches have been published [8-23]. At the initial stage, two-dimensional (2D) modeling method was employed in the research to predict the heat transfer and flow patterns inside the plasma torch [9-13]. The predicted arc voltage of the torch in the turbulent regime is much higher than the measured value; in addition the predicted axial location of the arc attachment at the anode surface is also much farther downstream than that observed in experiments [14]. With the rapid development of computer technology, the calculation of heat transfer and fluid flow for a 3D thermal plasma torch with axisymmetrical geometries become feasible [14-23]. The models most frequently used for simulations of plasma spray torches rely on the LTE approximation, and regard the plasma flow as a property-varying electromagnetic reactive fluid in chemical equilibrium state, in which the internal energy of the fluid is characterized by the single parameter of gas temperature [14-22]. Selvan et al. developed a steady 3D LTE model to describe the temperature and velocity distributions inside a DC plasma torch. Moreover the arc length and radius were also discussed. But the model overestimated the plasma gas temperature near the arc-root due to the assumption that all the electric current transferred to the anode only through a fixed arc-root [15-16]. Klinger L. et al. also developed a steady 3D LTE model simulation of the plasma arc inside a DC plasma torch. However, the position of the arc-root was determined arbitrarily [17]. A. Vardelle and J. P. Trelles developed a time-dependent 3D LTE model representing the fluctuations of plasma arc [18-22]. The voltage drop for the LTE model was larger compared with the experimental ones due to the hypothesis of LTE. A non-equilibrium (NLTE) model was developed for the non-transferred arc plasma torch, which showed better agreement with the experimental results [23]. However, to solve the NLTE model is extremely difficult due to the fact that the two-temperature chemical equilibrium needs to be considered compared with the LTE mode.

Due to the LTE assumptions for the conventional LTE mode, the value of electron temperature is equal to heavy particles temperature, which is low near the electrodes, especially near the anode surface. Hence the equilibrium electrical conductivity, being a function of electron temperature, is extremely low, which limits the flow of electrical current through the electrodes. To alleviate this, some additional assumptions are necessary to achieve high electrical conductivity near the electrodes. In the current study, a nominal electron temperature was proposed, that was derived from the plasma gas temperature and adjusted by the electrical field strength, to amend the electrical conductivity of plasma gas. Therefore, no more additional assumptions are necessary to ensure the electrical current path between the cathode and anode if the electrical conductivity of plasma gas is determined by the nominal electron temperature instead of the gas temperature.

In order to differentiate from the conventional LTE model, the model using this study was named “improved LTE model”. With the improved LTE model, the plasma gas temperature and velocity distributions inside a DC plasma torch were calculated, and the distributions of electrical potential and current density were investigated. The results show that the total voltage drop and the location of anode erosion obtained by the improved LTE model are well consistent with experimental observations.

II. DESCRIPTION OF THE MATHEMATICAL MODEL

A. Model Assumptions

The model developed in this study is based on the following main assumptions for simulating the heat transfer and flow patterns inside a plasma torch.

(1) The continuum assumption is valid and the plasma can be considered as a compressible gas in the state of Local Thermodynamic Equilibrium (LTE).
(2) The plasma is optically thin.
(3) Gravitational effect and viscous dissipation are considered negligible.
(4) The induced electric field is negligible in comparison with the applied electric field intensity in the plasma arc region.
(5) The variation of gas pressure inside the torch is so little that the effects of pressure on the thermodynamic and transport properties of plasma are negligible. Based on the LTE assumption, the thermodynamic and transport properties of plasma gas (such as c_p, μ and λ) are determined by the gas temperature excluding the electrical conductivity (σ) as mentioned above. The electrical conductivity of plasma gas is determined by the nominal electron temperature derived from gas temperature, corrected by the electric field.

B. Governing Equations

Based on the forgoing assumptions, the governing equations for a 3D time-dependent flow of arc plasma can be written as follows:

Conservation of mass:

$$\partial \rho \partial t + \nabla \cdot \rho V = 0 \quad (1)$$

Conservation of momentum:

$$\rho \partial V \partial t + V.\nabla V = j \times B - \nabla P + 2\,3\,\mu \nabla \cdot V + 2\nabla \cdot \mu S \quad (2)$$

Conservation of energy:

$$\rho cp \partial T \partial t + V.\nabla T - DPDt = j.E - Sr + \nabla \cdot \lambda \nabla T \quad (3)$$

Maxwell electromagnetism equations:

$$\nabla \cdot -\sigma \nabla \varnothing = 0 \quad (4)$$

$$E = -\nabla \varnothing \quad (5)$$

$$\Delta A = -\mu 0 j \quad (6)$$

$$B = \nabla \times A \quad (7)$$

Ohm law:

$$j = \sigma E \quad (8)$$

Density of plasma:

$$\rho = PRgT \quad with \quad Rg = k(nh + nenh mh + neme)$$

(9)

In order to determine the electrical conductivity of plasma gas, the electron temperature must be calculated. It is difficult to solve the electron energy conservation equation to get the electron temperature because of strong nonlinearity. Therefore, a nominal electron temperature was calculated from the equation as follows [24]:

$$Te-TTe=3\pi 32m\hbar mee\lambda eE32kTe2$$

(10)

C. Computational Domain and Boundary Conditions

The geometry used in the current study corresponds to the SG-100 plasma torch from Praxair. The cross sectional dimension of SG-100 torch used in this study is shown in figure 2 (a), and the 3D computational domain is shown in figure 2 (b). The computational domain is meshed using 217600 structured hexahedral cells with 224567 nodes as shown in the figure 2 (b).

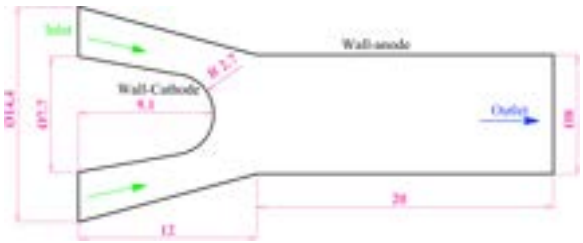

(a) Cross section dimension of SG-100 torch

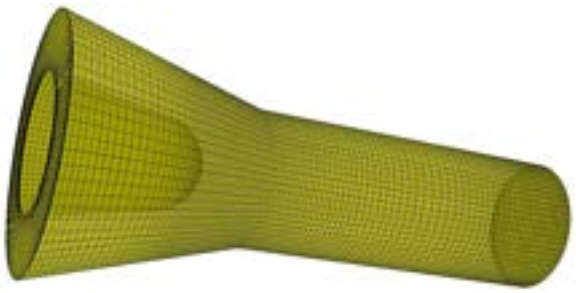

(b) Mesh of computational domain

Fig. 2. Geometry of the computational domain

As seen in figure 2, the boundary of the computational domain is divided into 4 different faces to allow the specification of boundary conditions. Table 1 shows the boundary conditions used in the simulation, where P_{in} represents the inlet pressure equal to 111325 Pa (10 kPa overpressure), h_w the convective heat transfer coefficient at the anode wall equal to 2×10^4 W.m^{-2}.K^{-1} [19-23], and T_w a reference cooling water temperature of 500 K. The electrical current density and temperature of the cathode was defined by:

$$jr=Jcat\hbar 0\exp -rRcnc \quad (11)$$

$$Tr=500+3000\exp -r2Rcnc \quad (12)$$

where r is radial distance from the torch axis ($r2=x2+y2$), and J_{cath0} and n_c are parameters that specify the shape of the current density profile. The R_c is calculated to ensure that integration of $j(r)$ over the cathode equals the total applied current. According to references 20 and 23, the values of the shape parameters used in the current study are shown in table 2.

Argon gas was employed as the plasma gas in this study. The conditions for simulation are shown in table 3.

Table 1. Boundary conditions

	Inlet	Cathode	Anode	Outlet
P	P_{in}	$\partial P\partial n=0$	$\partial P\partial n=0$	101325
V	Flow Rate	0	0	$\partial Vi\partial n=0$
T	300	$T(r)$	$Qa=\hbar w(T-Tw)$	$\partial T\partial n=0$
ø	$\partial ø\partial n=0$	$j(r)$	0	$\partial ø\partial n=0$
A	0	$\partial Ai\partial n=0$	$\partial Ai\partial n=0$	$\partial Ai\partial n=0$

Table 2. The shape parameters of current density

Specified Current (A)	J_{cath0} (A/m^2)	n_c	R_c (mm)
600	2.5e8	4	0.912245

Table 3. The conditions for simulation

Gas type	Applied current (A)	Gas flow rate (SLM)
Argon	600	50

The gas flow inside the plasma torch was calculated by FLUENT, commercial CFD software, with the SIMPLE algorithm. For gas flow calculations, the K-ε model is employed in this study.

Base on the assumption above, the electrical conductivity of plasma gas depends on gas electron temperature. The calculated method of electrical conductivity was presented in Ref. 23 and 25 to 27. The electrical conductivity of argon plasma gas in relation to the electron temperature is shown in figure 3. The other thermodynamic and transport properties of the plasma gas that only rely on the gas temperature, such as heat specific, thermal conductivity, viscosity and volumetric radiation, are taken from Ref. 28.

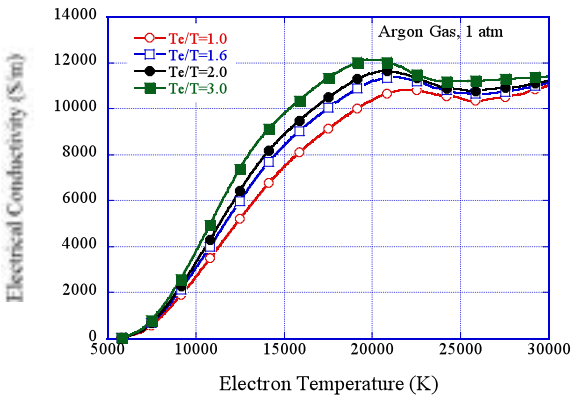

Fig. 3. Electrical conductivity of argon plasma gas [23, 25 and 26]

III. RESULTS AND DISCUSSIONS

A. Nominal electron temperature

Based on equation 10, the calculated nominal electron temperature of the argon gas in relation to different electric field strengths at the pressure of 1 atm is shown in figure 4. It's revealed that the high electric field strength prevents the establishment of an equilibrium state in which the gas temperature is equal to the electron temperature. Therefore, the nominal electron temperature is much higher than the gas

temperature especially under the low gas temperature conditions while the electric field strength is strong. In contrast, the nominal electron temperature is similar to the gas temperature while the electric field strength is low, due to few ionizations occurring. When the gas temperature is high enough to obtain sufficient collisions between the heavy particles and the electrons, the nominal electron temperature is also similar to the gas temperature with little dependency on the electric field strength as shown in the figure 4.

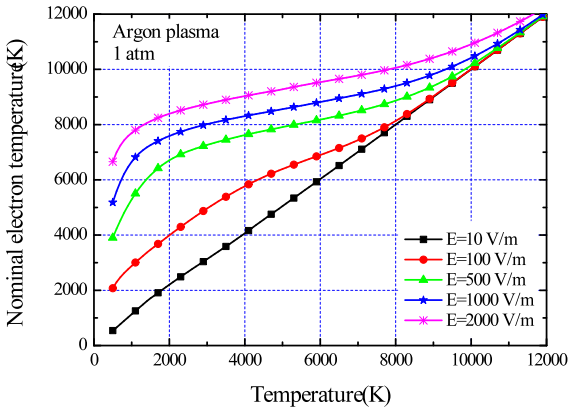

Fig. 4. The relationship between the nominal electron temperature and the gas temperature under different electric field strength

B. Flow fields inside the torch

Figure 5 (a) shows the voltage drop of the plasma column calculated by the improved LTE model. The amplitude of voltage is between 22 and 25 V with a fluctuation frequency of 13.9 kHz. An experiment was carried out to measure the plasma system power source voltage under the same conditions used in the current simulation, 600 A electrical current and 50 SLM gas flow rate. Limited by the experimental equipment, only the average voltage of power source was obtained. The experimentally observed voltage of the power source is 29.5 V. There are two reasons that the voltage drop calculated is lower than the experimental results. One is that the voltage drop of the plasma column should be less than voltage drop of plasma torch because the sheath voltage drop of the electrode was not taken into account in the simulation. The other is that the experimental voltage of the power source should be higher than the voltage drop of plasma torch owing to the voltage drop on the electrical cables. Figure 5 (b) shows the voltage drop of a SG-100 plasma torch researched by Trelles et al under the conditions of 700A electrical current and 60 SLM gas flow rate [23]. It seems that the experimental voltage drop in the reference 23 is a little lower than the ones in this study in spite of the higher electrical current applied. This is caused by the cable voltage drop in the current study because the voltage in reference 23 is the voltage drop of plasma torch instead of power source. The research reveals that voltage drop calculated with the LTE model is more than twice that of the experimental results. It seems that the improved LTE mode can obtain comparable accuracy to the NLTE mode.

The instantaneous temperature distributions inside the torch at 600 and 630μs, two representative times for observing the conditions at maximum and minimum voltage drop, are presented in figure 6. It can be observed that the distributions are almost axisymmetrical and the temperature of the plasma core is near 36500K at the current simulation conditions. The gas temperature distribution changes slightly with the elapse of time. Figure 7 shows the instantaneous velocity distribution inside the torch. Similar to the temperature distribution, the distribution of gas velocity is almost axisymmetrical. The maximum velocity of inside the torch is near 1740 m/s and the variation of velocity with the elapse of time is significant compared with the gas temperature.

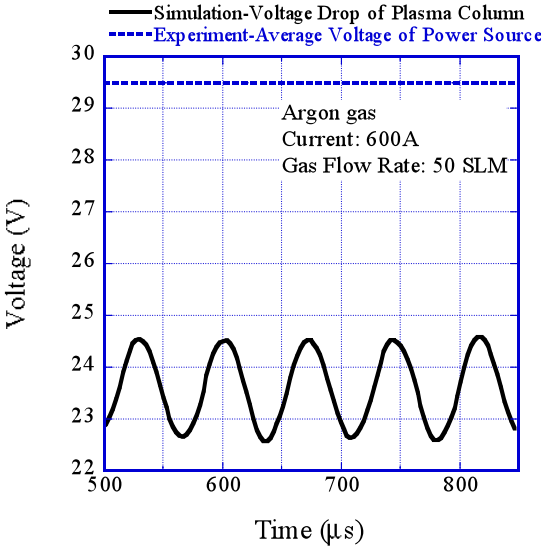

(a) Results in this study

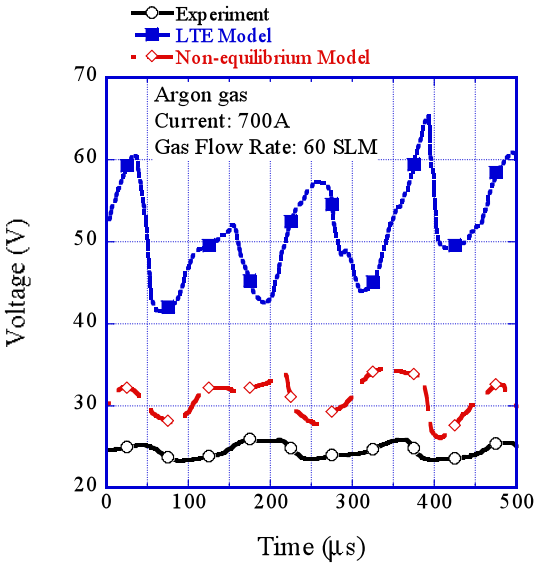

(b) Trelles's results in reference 23

Fig. 5. Voltage drop of plasma

Figure 8 and 9 show the gas temperature and velocity distributions of different axial cross sections inside the torch. It reveals that the distribution of gas temperature and velocity are almost axisymmetrical at all the axial cross sections.

The calculated nominal electron temperature distribution inside the torch is presented in figure 10. Compared to the gas temperature distribution in figure 6 (b), it is obviously higher than the gas temperature with greatly varying degrees depending

on the regions. As figure 4 shows, in the high temperature region near the plasma core, the nominal electron temperature is similar to the gas temperature owing to sufficient collisions between electrons and heavy particles under the condition of higher gas temperature. However, a significant difference between the nominal electron temperature and gas temperature is observed in the region far from the plasma core, especially the regions near the corner of the anode internal surface, where the nominal electron temperature is more than 10000 K. This is on account of the insufficient collisions between the electrons and the heavy particles in the lower gas temperature regions resulting in a great temperature difference. Consequently, the electrical current can reach the anode in spite of the lower gas temperature near the anode boundary because of the higher electrical conductivity determined by the nominal electron temperature. Therefore, the problem of lower electric conductivity near the anode boundary in the conventional LTE model can be solved in this study by calculating nominal electron temperature. Using the improved model, the simulation can be executed without making further assumptions about the electric conductivity.

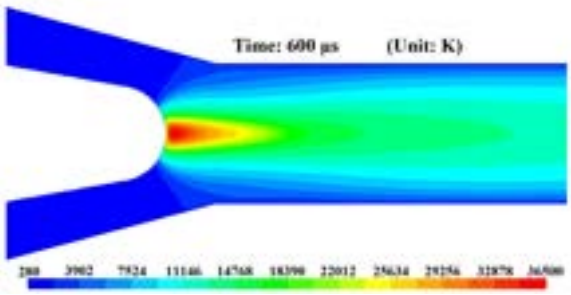

(a) at 600 μs

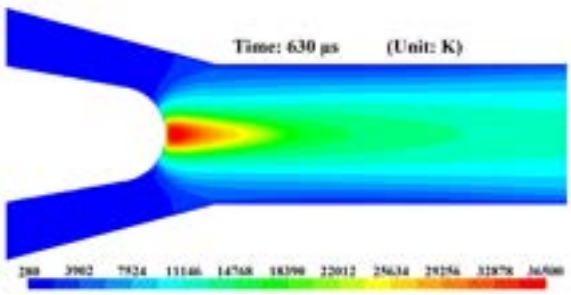

(b) at 630 μs

Fig. 6. Temperature distributions of a cross section inside the torch (unit: K)

Figure 11 shows the electric potential distribution inside the torch. It seems that different electrical potential is obtained along the cathode boundary although a uniform electric potential is loaded on the cathode. The minimum electrical potential of the plasma gas is observed at the cathode tip and the electrical potential should decrease with the increase of distance from the cathode tip. The situation is caused by the sheath voltage of the cathode, not considered in the current study. Therefore, the magnitude of the gas electrical potential at the cathode boundary should be the value of the plasma voltage subtracting the sheath voltage drop. According to the studies of Benilov and Zhou, higher temperature and electric current density lead to a lower sheath voltage drop [29-30]. Therefore, different electrical potential is observed at the cathode boundary because of the different sheath voltage drop.

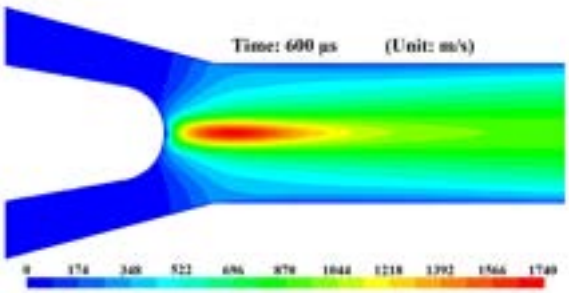

(a) at 600 μs

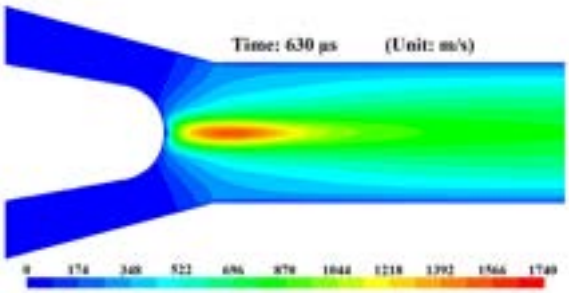

(b) at 630 μs

Fig. 7. Velocity distributions of a cross section inside the torch (unit: m/s)

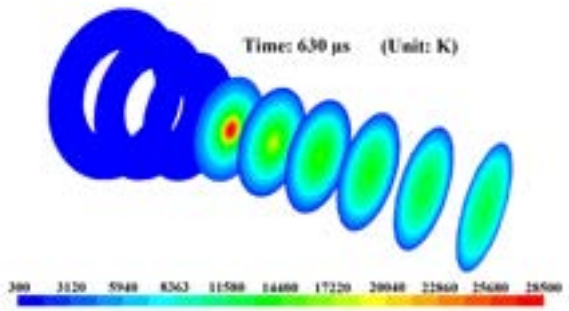

Fig. 8. Temperature distribution inside the torch of different axial cross sections at 630 μs (unit: K)

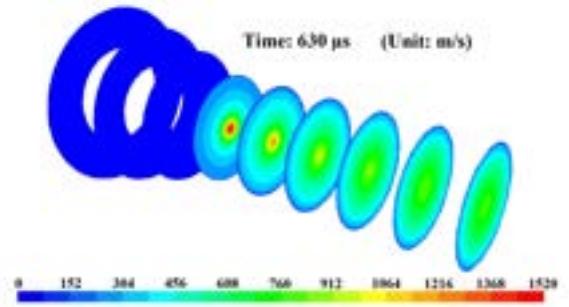

Fig. 9. Velocity distribution inside the torch of different axial cross sections at 630 μs (unit: m/s)

C. Gas flow at the torch exit

Figure 12 and 13 show the respective gas temperature and velocity distributions at the torch exit. The distributions of temperature and velocity are both axisymmetrical, the temperature at the symmetrical center of the torch exit is near 13000 K, and the velocity there is about 1000 m/s. It can be seen that the gas temperature and velocity of the torch exit at the time of 600 μs are a little higher than the ones at the time of 630 μs owing to the higher voltage drop of arc column as shown in Fig. 5 (a) resulting in a higher plasma power. This is evidence that the arc length is longer at the time of 600 μs than that of 630 μs.

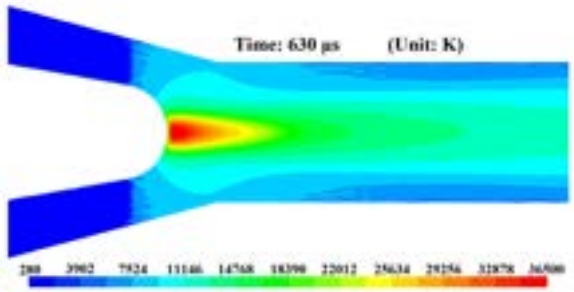

Fig. 10. Nominal electron temperature distribution of a cross section inside the torch at 630 μs (unit: K)

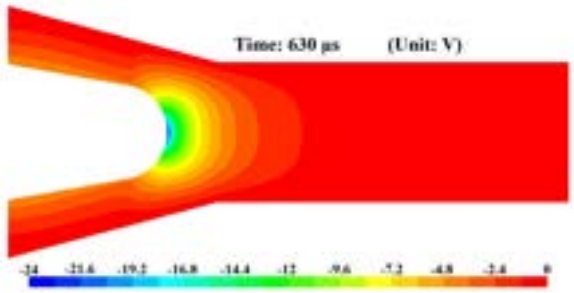

Fig. 11. Electric potential distribution of a cross section inside the torch at 630 μs (unit: V)

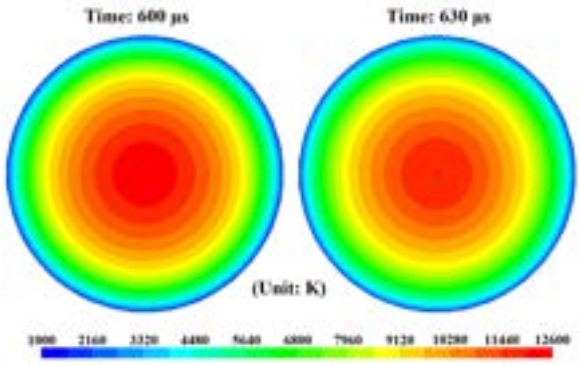

Fig. 12. Temperature distributions at the torch exit (unit: K)

Figure 14 shows the velocity and gas flow rate at the symmetrical center of the torch exit. It reveals that the gas velocity of the symmetrical center at the torch exit fluctuated periodically from 650 to 1000 m/s. The fluctuation of gas velocity at the symmetrical center of the torch exit is caused by the plasma arc fluctuation because the frequency is 13.9 kHz, similar to the fluctuation frequency of plasma voltage. The gas velocity fluctuation leads the gas flow rate at the torch exit to fluctuate around 50 SLM, the inlet flow rate, as shown in the figure 14 (b).

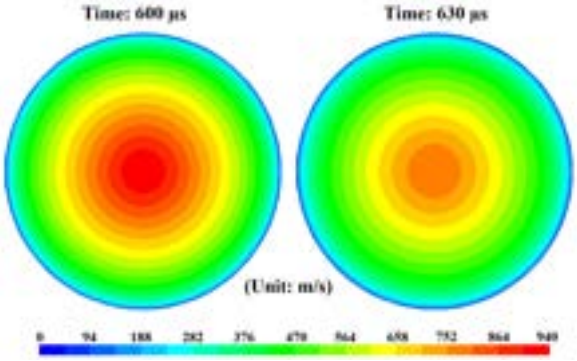

Fig. 13. Velocity distributions at the torch exit (unit: m/s)

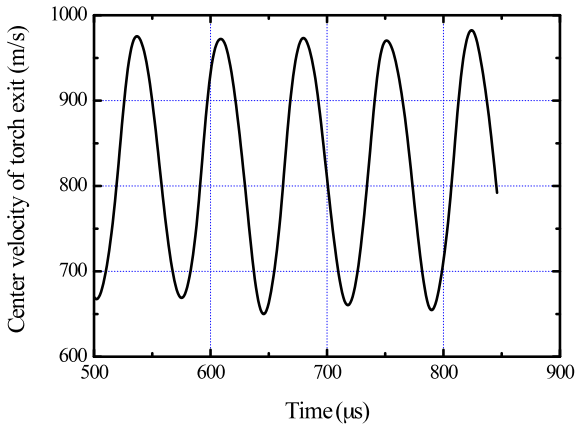

(a)

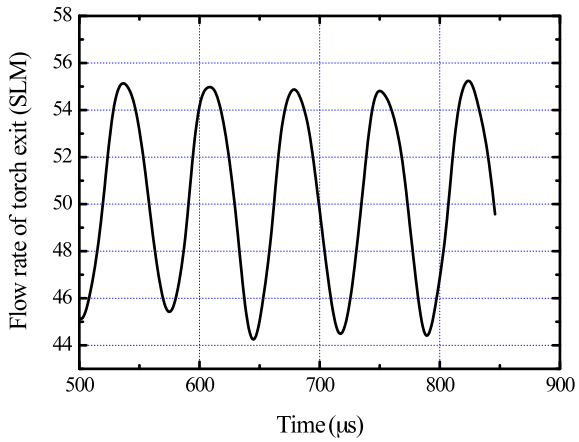

(b)

Fig. 14. (a) symmetrical center velocity and (b) gas flow rate of the torch exit

D. Erosion of the anode

An anode erosion test was carried out to ascertain location of erosion. In order to accelerate the rate of erosion, the conditions for the anode erosion test are somewhat different from the simulation conditions, as shown in table 4. The applied electrical current was increased to 750 A, and helium was mixed with

argon gas to raise the plasma voltage. Figure 15 shows two cross sections of used SG-100 torch's anodes. In Fig. 15 (a), the anode was used for 30 hours, and some slight erosion occurred at the anode internal surface. After extended usage, the anode was severely eroded as shown in figure 15 (b). It seems that anode erosion always occurs at the location close to the corner of the anode internal surface. Extended usage only leads to a spread of the erosion range.

Table 4. Spray conditions for anode erosion test

Argon flow rate (SLM)	50
Helium flow rate (SLM)	20
Electrical current (A)	750
Voltage (V)	40
Cooling water flow rate (l/min)	22-24

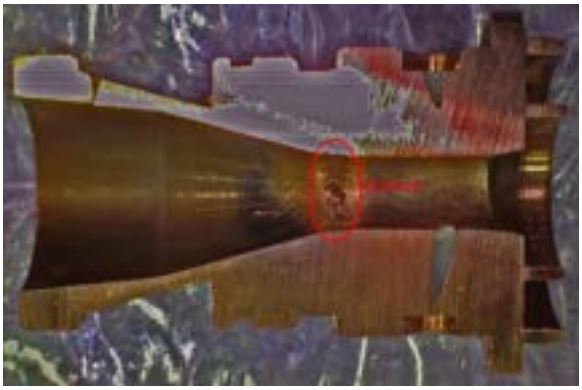

(a) Slight erosion for a relatively short time usage

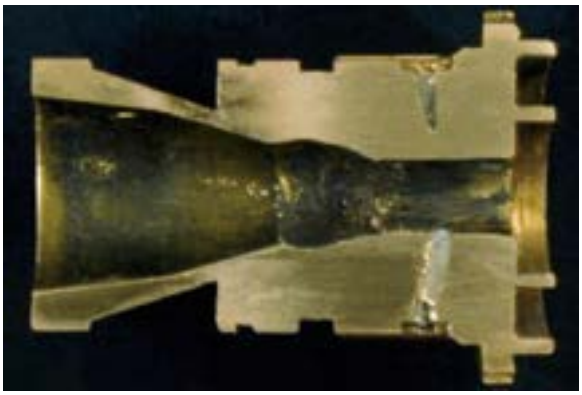

(b) Severe erosion for a relatively long time usage

Fig. 15. Eroded anode

Figure 16 shows the electric current density distributions inside the torch. It can be seen that the arc length at the time of 600 μs is longer than the one at the time of 630 μs. For a non-transferred DC plasma torch, the arc length depends on the balance of flow drag force and electromagnetic force. If the flow drag force dominates over electromagnetic force, the arc length becomes longer and the electromagnetic force increases. If the opposite occurs, the arc length will become shorter (ref 20). The arc length change leads to arc voltage fluctuation because a longer arc can gain high plasma voltage as shown in Fig 5 (a). Even though the arc length changes with time as shown in Fig. 16 (a), the similar location in the internal surface of anode is obtained, where the main electrical current passes through. It seems that the location is well consistent with the place of erosion. Overlapping the electrical current density distribution and the eroded anode reveals that the location of anode erosion is where the main electric current "path" passes through as shown in figure 16 (b).

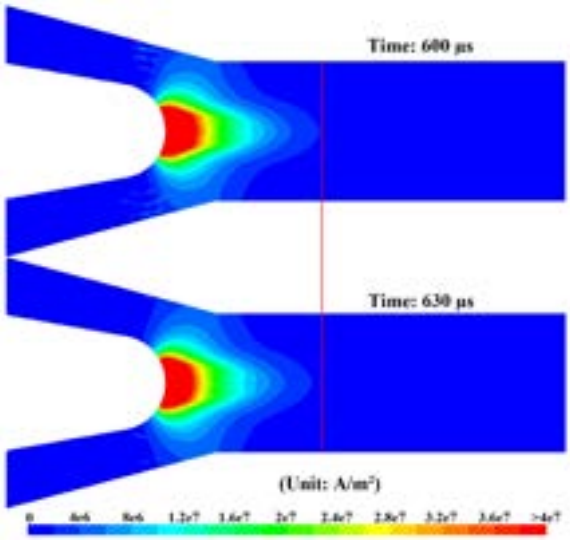

(a)

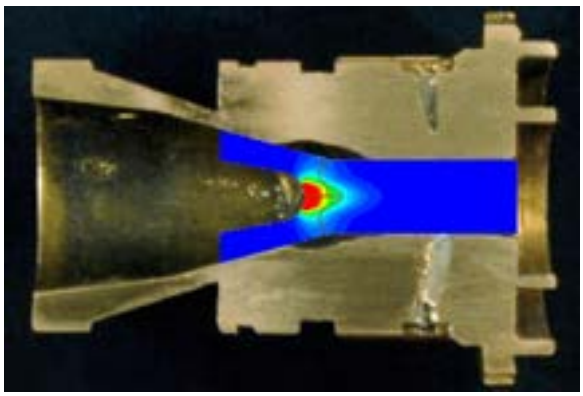

(b)

Fig. 16. Electric current density distribution of a cross section inside the torch (a) and overlapped with the eroded anode (b)

IV. CONCLUSIONS

An improved LTE model has been developed and applied to the three-dimensional and time-dependent simulation of the flow inside a DC arc plasma torch. The important change compared with the conventional LTE model is to adjust the electrical conductivity of plasma gas with a nominal electron temperature instead of the gas temperature. The temperature and velocity distribution of arc gas inside the torch were calculated, and the flow will fluctuate with the elapse of time. A gas temperature of about 13000K and velocity of about 1000 m/s were obtained at the torch exit. The voltage drop of arc column calculated matches well with the value measured. The location of anode erosion can also be predicted correctly using this model by the calculation of electric current density distribution.

REFERENCES

[1] P Fauchais, Understanding plasma spraying, J. Phys. D: Appl. Phys. 37 (2004) R86–R108

[2] T. Streibl, A. Vaidya, M. Friis, V. Srinivasan and S. Sampath, A critical assessment of particle temperature distributions during plasma spraying: experimental results for YSZ, Plasma Chemistry and Plasma Processing, Vol. 26, No. 1, February 2006, p73–102

[3] Z. Duan and J. Heberlein, Arc Instabilities in a Plasma Spray Torch, Journal of Thermal Spray Technology, Volume 11(1) March 2002, p44-51

[4] D. Outcalt, M. Hallberg, G. Yang, J. Heberlein, E. Pfender, P. Strykowski , Instabilities in Plasma Spray Jets, Proceedings of the 2006 International Thermal Spray Conference, May 15–18, 2006, Seattle, Washington, USA Copyright 2006 ASM International (In CD)

[5] J. F. Coudert, M. P. Planche, P. Fauchais, Characterization of DC Plasma Torch Voltage Fluctuations, Plasma Chemistry and Plasma Processing, Vol. 16, No. 1, 1996 (Supplement, 211S~227s)

[6] R. Ramasamy and V. Selvarajan, Current-voltage characteristics of a non-transferred plasma spray torch, Eur. Phys. J. D 8, p125–129

[7] S. Goutier, E. Nogues-Delbos, M. Vardelle, and P. Fauchais, Particle temperature fluctuations in plasma spraying, Journal of Thermal Spray Technology, Volume 17(5-6) Mid-December 2008, p895-901

[8] J.P. Trelles, C. Chazelas, A. Vardelle, and J.V.R. Heberlein, Arc Plasma Torch Modeling, Journal of Thermal Spray Technology, Volume 18, Numbers 5-6, p728-752

[9] R. Westhoff, A. H. Dilawari, J. Szekely, A Mathematical Representation of Transport Phenomena Inside a Plasma Torch, J. Appl. Phys., 1991, 190, p213-219

[10] Westhoff, R.; Szekely, J., A Model of Fluid, Heat Flow, and Electromagnetic Phenomena In a Nontransferred Arc Plasma Torch, Journal of Applied Physics, Volume 70, Issue 7, October 1, 1991, p3455-3466

[11] Han Peng, Yu lan, Chen Xi, Modeling of Plasma Jets with Computed Inlet Profiles, In: C.K. Wu, Editor, Proceedings of the 13th International Symposium on Plasma Chemistry, Peking University Press, Beijing (1997), p338–343

[12] Scott, D. A.; Kovitya, P.; Haddad, G. N., Temperatures in the Plume of a DC Plasma Torch, Journal of Applied Physics, Volume 66, Issue 11, December 1, 1989, p5232-5239

[13] Seungho Paik, P. C. Huang, J. Heberleinand and E. Pfender, Determination of the Arc-root Position in a DC Plasma Torch, Plasma Chemistry and Plasma Processing, Volume 13, Number 3, p379-397

[14] He-Ping Li and E. Pfender, Three Dimensional Modeling of the Plasma Spray Process, Journal of Thermal Spray Technology, Volume 16(2) June 2007, p245–260

[15] B. Selvan and K. Ramachandran, Comparisons Between Two Different Three-Dimensional Arc Plasma Torch Simulations, Journal of Thermal Spray Technology, Volume 18(5-6) Mid-December 2009, p 846–857

[16] B. Selvan, K. Ramachandran, K. P. Sreekumar, T. K. Thiyagarajan2, P. V. Ananthapadmanabhan, Three-Dimensional Numerical Modeling of an Ar-N2 Plasma Arc Inside a Non-Transferred Torch, Journal Plasma Science and Technology, IssueVolume 11, Number 6, p679-687

[17] Klinger L, Vos JB, Appert K, High-resolution CFD simulation of a plasma torch in 3 dimensions, Centre de Recherches en Physique des Plasmas – Preprint Report, LRP 763, http://crppwww.epfl.ch/

[18] C. Baudry, A. Vardelle, G. Mariaux, F C. Delalondre, Chatou, E. Meillot, Three-dimensional and time-dependent model of the dynamic behavior of the arc in a plasma spray torch, Thermal Spray 2004: Advances in Technology and Applications (ASM International), p717 – 723

[19] E. Moreau, C. Chazelas, G. Mariaux and A. Vardelle, Modeling the Restrike Mode Operation of a DC Plasma Spray Torch, Journal of Thermal Spray Technology, Volume 15, Number 4, p524-530

[20] J P Trelles, E Pfender and J V R Heberlein, Modelling of the arc reattachment process in plasma torches, Journal of Physics D: Applied Physics, Volume 40, Number 18, p5635

[21] Juan Pablo Trelles, Emil Pfender, Joachim Heberlein, Multiscale Finite Element Modeling of Arc Dynamics in a DC Plasma Torch, Plasma Chem Plasma Process (2006) V26, p557-575

[22] J. P. Trelles and J. V. R. Heberlein, Simulation results of Arc Behavior in Different Plasma Spray Torches, Journal of Thermal Spray Technology, Volume 15, Number 4, p563-569

[23] J P Trelles, J V R Heberlein and E Pfender, Non-equilibrium Modelling of Arc Plasma Torches, Journal of Physics D: Applied Physics, Volume 40, Number 19, p5937

[24] M. F. Zhukov and I. M. Zasypkin, Thermal Plasma Torches: Design, Characteristics, Application, Cambridge Int Science Publishing, 2007, p3

[25] V. Colombo, E. Ghedini, P. Sanibondi, Thermodynamic and transport properties in non-equilibrium argon, oxygen and nitrogen thermal plasmas, Progress in Nuclear Energy, V50 (2008), p921–933

[26] V Rat, P Andre, J Aubreton, M F Elchinger, P Fauchais and D Vacher, Transport coefficients including diffusion in a two-temperature argon plasma, J. Phys. D: Appl. Phys, 35 (2002) , p981–991

[27] V. Rat,P. Andre, J. Aubreton, M. F. Elchinger,P. Fauchais and A. Lefort, Transport properties in a two-temperature plasma: Theory and application, Physical Review E, V64, 026409

[28] Maher I. Boulos, Pierre Fauchais, Emil Pfender, Thermal plasmas: fundamentals and applications, Springer, 1994

[29] M S Benilov, Understanding and modelling plasma-electrode interaction in high-pressure arc discharges: a review, J. Phys. D: Appl. Phys. 41 (2008), p1-30

[30] X Zhou and J Heberlein, Analysis of the arc-cathode interaction of free-burning arcs, Plasma Source Sci. Technol. 3 (1994), p564-574

IEEE Transactions on Plasma Science; Volume: 39, Issue: 10, p 1974 – 1982